endolymphatic/perilymphatic space [9]. Recent advances in imaging technology enabled visualization of human endolymphatic hydrops by intratympanic Gd-DTPA administration at 3.0 T MRI [4–6]. The present study adds supportive evidence that endolymphatic hydrops can be diagnosed by the same protocol and expands the findings by semi-quantitative analysis. As in the previous reports [4–6], we could recognize the existence of endolymphatic hydrops as a decreased perilymphatic space, which may indicate an expanding endolymphatic space. Furthermore, semi-quantitative evaluation based on the ratio of the GBCA-enhanced area between affected/control sides represents the degree of endolymphatic hydrops.

In all 10 patients who had definite Meniere's disease, except for 1 (patient no. 4 with failure due to technical error), the ratio was reduced, and the quantitative ratio was 0.14 to 0.85. The present data are the first to indicate that bilateral intratympanic administration of GBCAs is beneficial in the semi-quantitative evaluation of endolymphatic hydrops.

There was inter-individual variation in the pattern of gadodiamide enhancement. For example, in patient no. 3, endolymphatic hydrops was predominantly detected in the cochlea (Figure 2). In contrast, vestibular hydrops was predominantly identified in patient no. 6 (Figure 3), in whom no VEMP response was found, suggesting that imaging findings are well correlated with the functional testing. A series of temporal bone studies also demonstrated that endolymphatic hydrops occurs either locally or entirely [10]. In the cochlea, the endolymphatic space is too small to recognize compared with the perilymphatic space, therefore endolymphatic space is usually undetected in the normal side. Thus, the existence of endolymphatic hydrops, which indicates abnormality, can be qualitatively identified more easily. In contrast, saccular endolymphatic spaces can be identified even in normal ears, making precise diagnosis for endolymphatic hydrops difficult without bilateral comparison. An additional advantage of the present procedure of bilateral intratympanic injection of a GBCA is the enablement of semi-quantitative comparison of endolymphatic space in the vestibule, which is difficult to evaluate by unilateral injection. In this study, four cases with definite MD showed significant differences in endolymphatic space in the saccular region and all of these patients (except patient no. 10 who could not be analyzed due to incomplete myogenic compression) showed decreased response. These correlations between imaging of sacculus associated with saccular functional testing such as VEMP will be of great help in precise diagnosis as well as therapeutic choice in MD.

In the present study, 6 of 11 patients who underwent caloric testing showed unilateral vestibular hypofunction. In comparison with VEMP, in some patients (nos 3, 8, and 12) both were decreased, but the others were shown to be abnormal in VEMP whereas normal in caloric responses (nos 1 and 3). Such discrepancy between the two testing methods, i.e. normal caloric test which is a function of the lateral semicircular canal, and a decrease in or disappearance of VEMP, has recently been reported in MD [11,12]. The present study confirms the saccular hydrops by imaging as well as VEMP, supporting the existence of such pathological conditions. In addition to general quantification, the advantage of bilateral intratympanic injection of GBCAs is semi-quantitative evaluation of saccular endolymphatic hydrops.

No adverse effects, such as vertigo, tinnitus, or hearing deterioration, were noted after intratympanic injection of gadodiamide, indicating that the present protocol can be safely performed in ordinary clinical settings. This is also supported by a recent study using guinea pigs in which diluted GBCAs had no apparent effects on endocochlear potential [13].

EcochG and glycerol testing have been widely performed as useful, but indirect, tests for the detection of endolymphatic hydrops in MD. Because these are indirect tests, EcochG or glycerol testing cannot play a decisive role in determining the presence or absence of endolymphatic hydrops. Unfortunately, in this study, systemic comparison between these tests and imaging results could not be performed. Therefore, a final conclusion concerning the relationship between these previous findings and the current MRI findings await future systemic comparative study.

The number of cases other than MD in this study was limited, and the etiology of each category of disease was not conclusive. In previous studies, 8.5% of patients with ALSNHL progressed to 'definite' MD [14], indicating that some MD was previously diagnosed as ALSNHL. In this study, the patient with ALSNHL was not associated with endolymphatic hydrops. Future study using many cases will subclassify ALSNHL whether it is associated with endolymphatic hydrops or not.

In this study, endolymphatic hydrops was also demonstrated in the patient with atypical MD who had fluctuated low frequency sensorineural hearing loss without vertigo, indicating the possibility that some atypical MD is a continuum clinical entity of MD. Therefore, in the future, the diagnostic criteria for MD may be expanded and reclassified according to image-based diagnosis.

In conclusion, bilateral intratympanic administration of a GBCA was successfully performed and

proved to be beneficial in the semi-quantitative evaluation of endolymphatic hydrops.

Acknowledgements

We thank Ms A.C. Apple-Mathews for help in preparing the manuscript. This study was supported by a Health Sciences Research Grant (Research on Eye and Ear Science, Immunology, Allergy and Organ Transplantation) from the Ministry of Health and Welfare of Japan and by the Acute Profound Deafness Research Committee of the Ministry of Health and Welfare of Japan.

Declaration of interest: The authors report no conflicts of interest. The authors alone are responsible for the content and writing of the paper.

References

[1] Sajjadi H, Paparella MM. Meniere's disease. Lancet 2008; 372:406–14.

[2] Committee on Hearing and Equilibrium. Committee on Hearing and Equilibrium guidelines for the diagnosis and evaluation of therapy in Meniere's disease. Otolaryngol Head Neck Surg 1995;113:181–5.

[3] Noguchi Y, Nishida H, Takano H, Kawashima Y, Kitamura K. Comparison of acute low-tone sensorineural hearing loss versus Meniere's disease by electrocochleography. Ann Otol Rhinol Laryngol 2004;113:194–9.

[4] Nakashima T, Naganawa S, Sugiura M, Teranishi M, Sone M, Hayashi H, et al. Visualization of endolymphatic hydrops in patients with Meniere's disease. Laryngoscope 2007;117: 415–20.

[5] Naganawa S, Satake H, Kawamura M, Fukatsu H, Sone M, Nakashima T. Separate visualization of endolymphatic space, perilymphatic space and bone by a single pulse sequence; 3D-inversion recovery imaging utilizing real reconstruction after intratympanic Gd-DTPA administration at 3 Tesla. Eur Radiol 2008;18:920–4.

[6] Naganawa S, Satake H, Iwano S, Fukatsu H, Sone M, Nakashima T. Imaging endolymphatic hydrops at 3 Tesla using 3D-FLAIR with intratympanic Gd-DTPA administration. Magn Reson Med Sci 2008;7:85–91.

[7] Koizuka I, Seo Y, Murakami M, Seo R, Kato I. Micromagnetic resonance imaging of the inner ear in the guinea pig. NMR Biomed 1997;10:31–4.

[8] Koizuka I, Seo R, Kubo T, Matsunaga T, Murakami M, Seo Y, et al. High-resolution MRI of the human cochlea. Acta Otolaryngol Suppl 1995;520:256–7.

[9] Zou J, Pyykko I, Bjelke B, Dastidar P, Toppila E. Communication between the perilymphatic scalae and spiral ligament visualized by in vivo MRI. Audiol Neurootol 2005;10: 145–52.

[10] Lin MY, Timmer FC, Oriel BS, Zhou G, Guinan ZZ, Guinan JJ, et al. Vestibular evoked myogenic potentials (VEMP) can detect asymptomatic saccular hydrops. Laryngoscope 2006;116:987–92.

[11] de Waele C, Huy PTB, Diard JP, Freyss G, Vidal PP. Saccular dysfunction in Meniere's disease. Am J Otol 1999; 20:223–32.

[12] Iwasaki S, Takai Y, Ito K, Murofushi T. Abnormal vestibular evoked myogenic potentials in the presence of normal caloric responses. Otol Neurotol 2005;26:1196–9.

[13] Kakigi A, Nishimura M, Takeda T, Okada T, Murata Y, Ogawa Y. Effects of gadolinium injected into the middle ear on the stria vascularis. Acta Otolaryngol 2008;128:841–5.

[14] Junicho M, Aso S, Fujisaka M, Watanabe Y. Prognosis of low-tone sudden deafness: does it inevitably progress to Meniere's disease? Acta Otolaryngol 2008;128:304–8.

Acta Oto-Laryngologica
2009, 1–4, iFirst article

informa
healthcare

CASE REPORT

Endolymphatic hydrops and therapeutic effects are visualized in 'atypical' Meniere's disease

MAIKO MIYAGAWA[1], HISAKUNI FUKUOKA[1], KEITA TSUKADA[1], TOMOHIRO OGUCHI[1], YUTAKA TAKUMI[1], MAKOTO SUGIURA[2], HITOSHI UEDA[3], MASUMI KADOYA[3] & SHIN-ICHI USAMI[1]

[1]*Department of Otorhinolaryngology and* [3]*Department of Radiology, Shinshu University School of Medicine, Matsumoto and* [2]*Department of Otorhinolaryngology, Kariya Toyota General Hospital, Kariya, Japan*

Abstract
A 53-year-old male with fluctuating low frequency sensorineural hearing loss and tinnitus, but without vertigo, was evaluated by MRI obtained by intratympanic injection of a gadolinium-based contrast agent (GBCA) before and after the administration of isosorbide. The endolymphatic hydrops was semi-quantitatively evaluated by a 3.0-T MR scanner. For quantification, the affected side/contralateral side ratios were calculated. A gadodiamide (a kind of GBCA)-enhanced space surrounding the endolymph in the affected side with a 0.50 ratio (which may have represented endolymphatic hydrops) improved after isosorbide therapy to a 0.98 ratio. Thus, endolymphatic hydrops was demonstrated in a patient with 'atypical' Meniere's disease (MD), suggesting that at least some atypical MD may share similar etiology with, and therefore be a continuum of, MD. Also, therapeutic effects could be visualized by using MRI. Therefore, MRI-based diagnosis of MD-related disease will be a powerful tool not only because of its precision but also its usefulness for therapeutic evaluation.

Keywords: *Atypical Meniere's disease, cochlear Meniere's disease, endolymphatic hydrops, MRI, gadolinium-based contrast agents (GBCAs), osmotic diuretics, isosorbide*

Introduction

Meniere's disease (MD) is an idiopathic disorder of the inner ear characterized by fluctuating sensorineural hearing loss (SNHL), tinnitus and aural fullness, and recurrent spontaneous episodic rotational vertigo (see Sajjahi and Paparella for review [1]).

Clinical diagnosis of MD has sometimes been hampered by the diagnostic criteria, because the full complement of symptoms does not develop simultaneously in some cases. These cases have been reported as so-called 'atypical' MD. 'Vestibular MD' is characterized by recurrent episodic vertigo but without hearing loss. In contrast, 'cochlear MD' is defined as having fluctuating low frequency hearing loss without vertigo [2,3].

Although, in 1995, the Committee on Hearing and Equilibrium of the American Academy of Otolaryngology-Head and Neck Surgery (AAO-HNS) limited the diagnostic term MD to those patients in whom the full complement of symptoms was present, functional testing results for atypical MD mimic classical MD [1]. For example, cochlear MD shows positive glycerol test and histopathologic findings similar to classical MD [2,3], and increased summating potential to eighth nerve action potential (SP/AP) was reported in vestibular MD [4,5]. On the basis of these findings, atypical MD is thought to be a continuum of MD but no additional supportive evidence has come to light for quite some time.

Recent advances in imaging by three-dimensional, fluid-attenuated inversion recovery (3D-FLAIR) of magnetic resonance imaging (MRI), in association with gadolinium-based contrast agents (GBCAs) enhancement, enables visualization of endolymphatic hydrops in patients with MD [6–8]. Interesting questions were 1) whether atypical MD is associated

Correspondence: Shin-ichi Usami, Department of Otorhinolaryngology, Shinshu University School of Medicine, 3-1-1 Asahi, Matsumoto 390-8621, Japan. Tel: +81 263 37 2666. Fax: +81 263 36 9164. E-mail: usami@shinshu-u.ac.jp

(Received 27 October 2008; accepted 30 October 2008)

ISSN 0001-6489 print/ISSN 1651-2251 online
DOI: 10.1080/00016480802593513

with endolymphatic hydrops or not, and 2) whether endolymphatic hydrops can be visualized by MRI. In the present study, we evaluated endolymphatic hydrops, found in cochlear MD, in a quantitative manner before and after osmotic diuretic therapy.

Case study

A 53-year-old male with fluctuating low frequency SNHL and tinnitus, but without vertigo (i.e. not fulfilling the AAO-HNS diagnostic criteria of MD) was evaluated audiologically and with MRI obtained by a 3.0-T scanner.

The patient had experienced hearing fluctuation without associated episodic vertigo four times from 2006 to 2008, and had been treated with steroids and osmotic diuretics. The audiogram and hearing fluctuation of this patient are summarized in Figure 1. Normal speech discrimination and the recruitment investigation tests including Bekesy audiometry and short increment sensitivity index (SISI) test confirmed that there was cochlear involvement. A positive glycerol test (10% glycerol 500 ml, intravenous administration for 2 h with hearing test performed before/after injection) suggested possible endolymphatic hydrops (Figure 2). Initial treatment was hydrocortisone sodium succinate (300 mg/day for 2 days, 200 mg/day for 2 days, 100 mg/day for 2 days) and isosorbide 90 ml/day for 6 days, and was followed by oral osmotic diuretics (isosorbide 90 ml/day) for 350 days.

For imaging study, the protocol described previously [6–8] was applied bilaterally. In brief, diluted gadodiamide (a kind of GBCA) was administered to the bilateral tympanic cavity by injection through the tympanic membrane. After 24 h, the endolymphatic hydrops was evaluated by MRI using a 3.0-T scanner. The areas enhanced by gadodiamide (a kind of GBCA) were measured by imaging analysis software, and the affected side/contralateral side ratios were calculated.

The perilymphatic space is enhanced by gadodiamide (a kind of GBCA), in contrast to the endolymphatic space, which is not. The endolymphatic space is comparatively small and difficult to identify as a vacant area in the normal side. In contrast, the endolymphatic space in an ear with endolymphatic hydrops is partially or entirely expanded, making identification of the endolymphatic space easier.

A reduced perilymphatic space surrounding the endolymph (which may have represented endolymphatic hydrops) was observed in this patient (Figure 3). The gadolinium-enhanced area representing the perilymphatic space ratio was reduced, and the quantitative ratio was 0.50 (Figure 2).

The patient gradually recovered hearing after 350 days and it was stabilized to symmetricity (Figure 3).

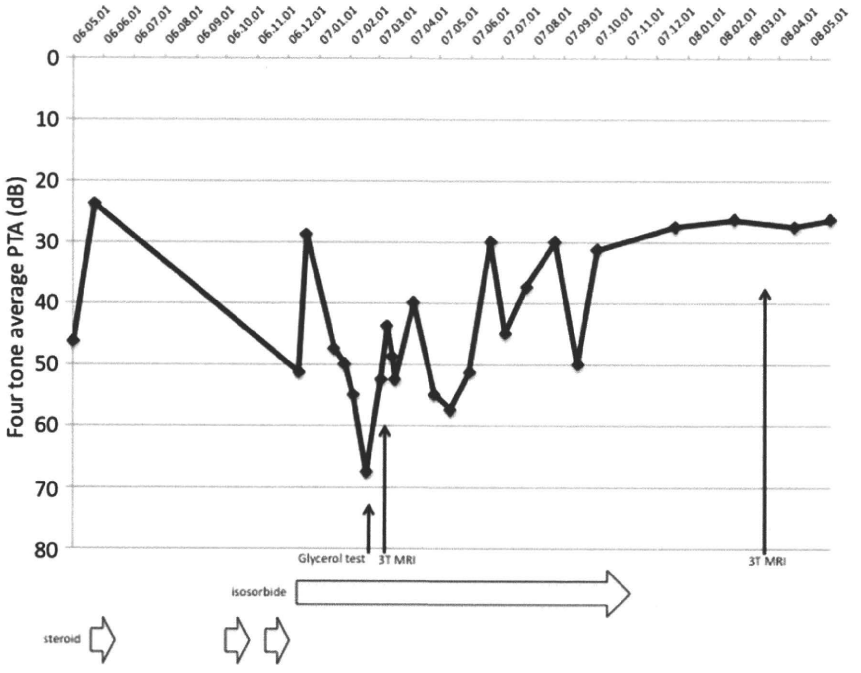

Figure 1. Time course of hearing level (four tone, 500, 1 K, 2 K, 4 K Hz average of pure tone audiometry) and therapeutic agents, indicating that hearing is fluctuated but gradually recovered after long-term osmotic diuretic therapy.

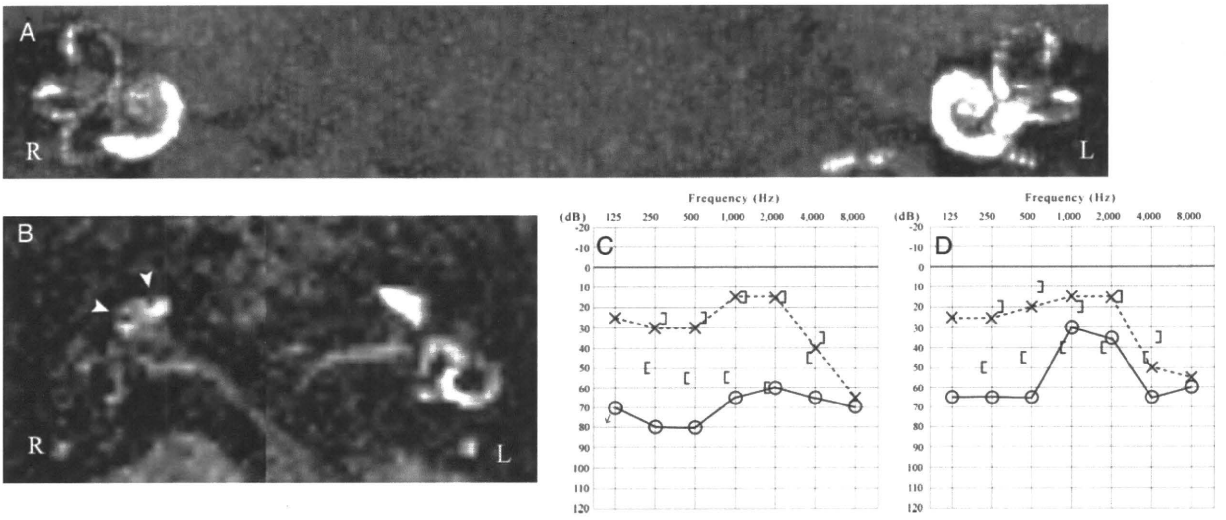

Figure 2. MRI before therapy. (A) The areas enhanced by gadodiamide in the cochlea and vestibule were measured using multi-planar reconstruction (MPR) image by imaging analysis software, and the affected side/unaffected side ratios were calculated. (B) The black area inside the perilymphatic space in the basal turn of the left cochlea that is filled with gadodiamide is the endolymphatic hydrops. On the contralateral side, the endolymphatic space is a significantly small area that is not detectable, likely because of the strong signal intensity in the perilymphatic space. (C, D) Pure tone audiogram: (C) before and (D) after glycerol test.

Discussion

As in definite MD [6–9], in this study, endolymphatic hydrops was demonstrated in an atypical MD patient, who did not fulfill the classical diagnostic criteria for MD, suggesting that at least some atypical MD may share a similar etiology with, and therefore be a continuum of, MD. This concept is supported by the observations that auditory and vestibular symptoms do not always occur simultaneously and the similarity in functional testing results [4]. A series of temporal bone studies also demonstrated that endolymphatic hydrops occurs either locally or entirely [10]. Against this background, recent MRI studies clearly showed inter-individual differences in regional predominance in hydrops; some cases are cochlear predominant whereas some are vestibular predominant. Such differences may lead to a diagnosis of atypical MD, which is a continuum category of disease, and therefore should be treated by the same protocol.

Although MD has been attributed to endolymphatic hydrops, only post-mortem histopathological confirmation has been available. Electrocochleography (EcochG), glycerol test, or other functional

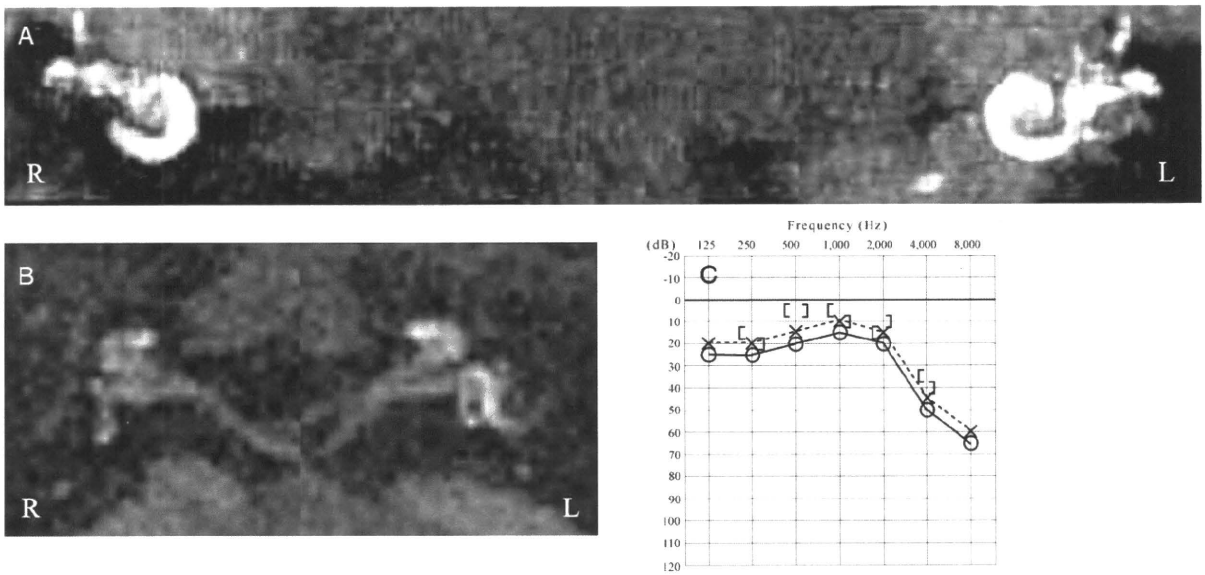

Figure 3. MRI imaging after therapy. (A, B) The area representing the perilymphatic space enhanced by gadodiamide is increased. (C) Hearing is recovered.

testing has been utilized to estimate endolymphatic hydrops, but these do not give direct proof [1]. These limited options of clinical diagnosis and functional testing were all that were available, thus making precise diagnosis of MD difficult.

Accordingly, visualization of endolymphatic hydrops by 3D-FLAIR of MRI, in association with GBCAs enhancement, will be a breakthrough, giving us a powerful tool to confirm endolymphatic hydrops.

The present imaging data demonstrated that cochlear MD is a continuum disease of classical MD; both being characterized by endolymphatic hydrops. Although further study will be necessary to reach any conclusions, in the near future the diagnostic criteria for MD may be reclassified according to image-based diagnosis.

Furthermore, this study is the first to successfully demonstrate the change in the degree of endolymphatic hydrops in the same subject before and after treatment. Quantitative analysis by bilateral administration of GBCAs with 3.0T-MRI is beneficial to such evaluation. Among several treatment choices, the present results demonstrated direct evidence of the change in endolymphatic hydrops, which may be due to the response to therapeutic agents, i.e. osmotic diuretics (isosorbide). Since the possibility remains that these results were a matter of a natural course, a further large cohort study will be necessary. However, this study demonstrated that MRI-based imaging has a great potential to be a powerful tool not only for precise diagnosis of MD and its variants, but also in therapeutic evaluation of endolymphatic hydrops.

Acknowledgements

We thank Ms A.C. Apple-Mathews for help in preparing the manuscript. This study was supported by a Health Sciences Research Grant (Research on Eye and Ear Science, Immunology, Allergy and Organ Transplantation) from the Ministry of Health and Welfare of Japan and by the Acute Profound Deafness Research Committee of the Ministry of Health and Welfare of Japan.

Declaration of interest: The authors report no conflicts of interest. The authors alone are responsible for the content and writing of the paper.

References

[1] Sajjahi H, Paparella MM. Meniere's disease. Lancet 2008; 372:406–14.

[2] Williams HL, Horton BT, Day LA. Endolymphatic hydrops without vertigo. Arch Otolaryngol 1950;51:557–81.

[3] Kohut RI, Lindsay JR. Pathologic changes in idiopathic labyrinthine hydrops. Acta Otolaryngol 1972;73:402–12.

[4] Paparella MM, Mancini F. Vestibular Meniere's disease. Otolaryngol Head Neck Surg 1985;93:148–51.

[5] Dornhoffer JL, Arenberg IK. Diagnosis of vestibular Meniere's disease with electrocochleography. Am J Otol 1993;14: 161–4.

[6] Nakashima T, Naganawa S, Sugiura M, Teranishi M, Sone M, Hayashi H, et al. Visualization of endolymphatic hydrops in patients with Meniere's disease. Laryngoscope 2007;117: 415–20.

[7] Naganawa S, Satake H, Kawamura M, Fukatsu H, Sone M, Nakashima T. Separate visualization of endolymphatic space, perilymphatic space and bone by a single pulse sequence; 3D-inversion recovery imaging utilizing real reconstruction after intratympanic Gd-DTPA administration at 3 Tesla. Eur Radiol 2008;18:920–4.

[8] Naganawa S, Satake H, Iwano S, Fukatsu H, Sone M, Nakashima T. Imaging endolymphatic hydrops at 3 Tesla using 3D-FLAIR with intratympanic Gd-DTPA administration. Magn Reson Med Sci 2008;7:85–91.

[9] Fukuoka H, Tsukada K, Miyagawa M, Oguchi T, Takumi Y, Suigiura M, Ueda H, Kadoya M, Usami S. Semi-quantitative evaluation of endolymphatic hydrops by bilateral intratympanic gadolinium-based contrast agent (GBCA) administration with MRI for Meniere's disease. Acta Otolaryngol (in press).

[10] Paparella MM. Pathology of Meniere's disease. Ann Otol Rhinol Laryngol Suppl 1984;112:31–5.

Clin Genet 2009: 75: 480–484
Printed in Singapore. All rights reserved

CLINICAL GENETICS
doi: 10.1111/j.1399-0004.2008.01138.x

Short Report

Factors that affect hearing level in individuals with the mitochondrial 1555A>G mutation

Lu SY, Nishio S, Tsukada K, Oguchi T, Kobayashi K, Abe S, Usami S. Factors that affect hearing level in individuals with the mitochondrial 1555A>G mutation.
Clin Genet 2009: 75: 480–484. © Blackwell Munksgaard, 2009

The mitochondrial 1555A>G mutation is one of the most common mutations responsible for hearing loss in Asians. Although the association with aminoglycoside exposure is well known, there is great variation in the severity of hearing loss. We analyzed hearing levels in 221 Japanese individuals with this mutation and attempted to identify relevant covariants including (i) age, (ii) aminoglycoside exposure, (iii) heteroplasmy ratio, and (iv) other gene mutations. At every age, average hearing levels were worse than those in normal subjects, suggesting that mitochondrial function itself may affect the severity of hearing loss. Although the hearing loss in individuals with the 1555A>G mutation progressed with age, the rate did not differ from that of the normal subjects. Those who had reported aminoglycoside exposure had moderate-to-severe hearing impairment regardless of age, confirming that such exposure is the most important environmental variable. We also confirmed the presence of heteroplasmy, which is known to modify the expression of other mitochondrial diseases, but found no evidence for a significant correlation with hearing impairment. A high prevalence of *GJB2* heterozygous mutations was noted, indicating that these mutations may exhibit epistatic interaction with the 1555A>G mutation.

SY Lu[a], S Nishio[a], K Tsukada[a], T Oguchi[a], K Kobayashi[a], S Abe[b] and S Usami[a]

[a]Department of Otorhinolaryngology, Shinshu University School of Medicine, Matsumoto, Japan, and [b]Division of Advanced Technology and Development, BML, Inc, Kawagoe-shi, Saitama, Japan

Key words: 12S rRNA – 1555A>G mutation – aminoglycosides – *GJB2* – hearing loss – mitochondria

Corresponding author: Shin-ichi Usami, MD, PhD, Department of Otorhinolaryngology, Shinshu University School of Medicine, 3-1-1 Asahi, Matsumoto 390-8621, Japan.
Tel.: +81 263 37 2666;
fax: +81 263 36 9164;
e-mail: usami@shinshu-u.ac.jp

Received 9 August 2008, revised and accepted for publication 20 October 2008

The 1555A>G mutation in the mitochondrial 12S rRNA gene (1) is the commonest mitochondrial mutation associated with hearing loss. Generally associated with aminoglycoside exposure (2, 3), there are also well-documented patients without a history of exposure (4–6). Systematic screening of Japanese hearing loss patients revealed that approximately 3–5% of these subjects had the 1555A>G mitochondrial mutation, and in those patients who had reported aminoglycoside exposure, the mutation was found in 33% (1, 7). This mutation has been found not only in patients with late-onset hearing loss but also in those with congenital/early-onset sensorineural hearing loss (8). The mitochondrial 1555A>G mutation has been considered to be transmitted in the homoplasmic state, but there have been recent reports of patients with heteroplasmy (8, 9). In an effort to prevent severe deafness, we distribute a drug use warning card advising avoidance of aminoglycosides to 1555A>G mutation family members who are not yet affected (10). The hearing impairment associated with aminoglycoside exposure is usually a bilateral, progressive, high-frequency sensorineural loss. Although it is clear that the patients who report a history of aminoglycoside exposure have a more severe hearing impairment, the severity of deafness is variable (4, 6), suggesting the contribution of additional factors. Age-related expression/progression of hearing loss is one possible factor (4, 5). The existence of modifier genes has also been postulated (11–14), although no candidate genes have been identified. Finally, it was also recently reported that heteroplasmy ratios of the mitochondrial 1555A>G mutation appear to be associated with phenotype variability (9). In order to clarify the possible involvement of these factors in the severity of hearing loss, we investigated the effect of (i) age, (ii) aminoglycoside exposure, (iii) heteroplasmy ratio, and (iv) other gene mutations in 221 individuals with the 1555A>G mutation.

Materials and methods

Subjects

The subjects in this study were 221 Japanese individuals from 67 families with the 1555A>G mutation, ranging in age from 2 months to 87 years. The number of affected members in individual families ranged from 1 to 24 with an approximate average of 3.3. The control group used to determine *GJB2* allele frequency was composed of 252 independent Japanese subjects with normal hearing.

Methods

Audiological analysis

Hearing level was classified using a pure-tone average over 500, 1000, 2000, and 4000 Hz in the better hearing ear. The hearing tests were performed at ages 4–87 years.

Mutation analysis

We screened for the 1555A>G mitochondrial DNA (mtDNA) mutation as described previously (4). In brief, total DNA including genome DNA and mtDNA was extracted from the blood, and the mitochondrial nucleotides 1252 through 1726 were amplified by polymerase chain reaction (PCR). To identify the *Alw*26I site, digestion was performed with a restriction enzyme (*Alw*26I). An ABI sequencer 3100XL (Perkin Elmer Co., Ltd, Waltham, MA) was used to confirm the 1555A>G mutation by direct sequencing.

To identify *GJB2* mutations, a DNA fragment containing the entire coding region was amplified using the primer pair Cx48U/Cx1040L (15). PCR products were sequenced and analyzed with an ABI sequencer 3100XL (Perkin Elmer Co., Ltd). [See Abe et al. (15) for details of the sequencing analysis methods.]

Heteroplasmy ratio of the 1555A>G mitochondrial mutation

The Hitachi FMBIO II image scanning machine (Hitachi Co., Ltd, Minatoku, Tokyo, Japan), a fluorescence imaging system, was used to quantify the heteroplasmy ratio by detection of fluorescently labeled and digested PCR products as described below. A 459 bp DNA fragment was amplified with Ex *Taq* DNA polymerase (Takara Bio Inc., Ohtsushi, Shiga, Japan) using 200 ng of DNA from the subject as a template. Primer sequences were as follows: upper primer, 5′- GCCTATATACCGCCATCTTC -3′; lower primer, 5′- TCTGGTAGTAAGGTGGAGTG -3′. The upper primer was fluorescently labeled at 5′ with rhodamine. PCR conditions were 95°C for 6 min, followed by 27 cycles of 95°C for 30 s, 55°C for 30 s and 72°C for 50 s and 72°C for 7 min. The PCR products were digested with restriction endonuclease *Alw*26I (Fermentas; 2.5 units, 37°C for 8–16 h). The subsequent PCR products were digested at 37°C for 8–16 h with 2.5 units of *Alw*26I (Fermentas). Two fluorescent products, wild type (300 bp) and/or mutant (459 bp), were detected because the 1555A>G mutation destroys the restriction site for *Alw*26I. The fluorescent intensity of the mutant bands in quantification experiments from two independent PCR amplifications was used to estimate the proportion of mutant copies in heteroplasmic subjects. We subcloned the insert including the 1555 position into the pDrive cloning vector using a QIAGEN PCR cloning kit (10) (QIAGEN, Hilden, Germany) as an appropriate standard of mutant heteroplasmy. The standard mixtures containing different amounts of wild-type and mutant synthesized oligonucleotides were used with analytical runs to quantify heteroplasmy of mtDNAs.

Statistical analyses

Student's *t*-test was used to compare average hearing levels of subjects with and without *GJB2* mutations and with and without aminoglycoside exposure.

Results

The hearing loss of individuals with the 1555A>G mutation progressed with age; however, the rate of progression did not differ from that found in the normal population (Fig. 1a). The aminoglycoside exposure group had moderate-to-severe hearing impairment regardless of age (Fig. 1b). The existence of heteroplasmy was confirmed in 10 individuals from eight families; however, no apparent correlation was found between heteroplasmy ratio and hearing loss severity (Fig. 1c). There was a high prevalence of *GJB2* heterozygous mutations in individuals bearing the 1555A>G mitochondrial mutation (Table 1), and their hearing levels tended to be worse (without *GJB2* mutation, 35.4 dB; with *GJB2* mutation, 42.0 dB), but the difference was not statistically significant (Fig. 1d). All the *GJB2* mutations found were in heterozygous state, and no subjects were associated with biallelic mutations. There was no correlation between mutation genotype and hearing level.

Discussion

The average hearing level in people with the 1555A>G mutation was worse than that in normal populations at any age (Fig. 1a). This

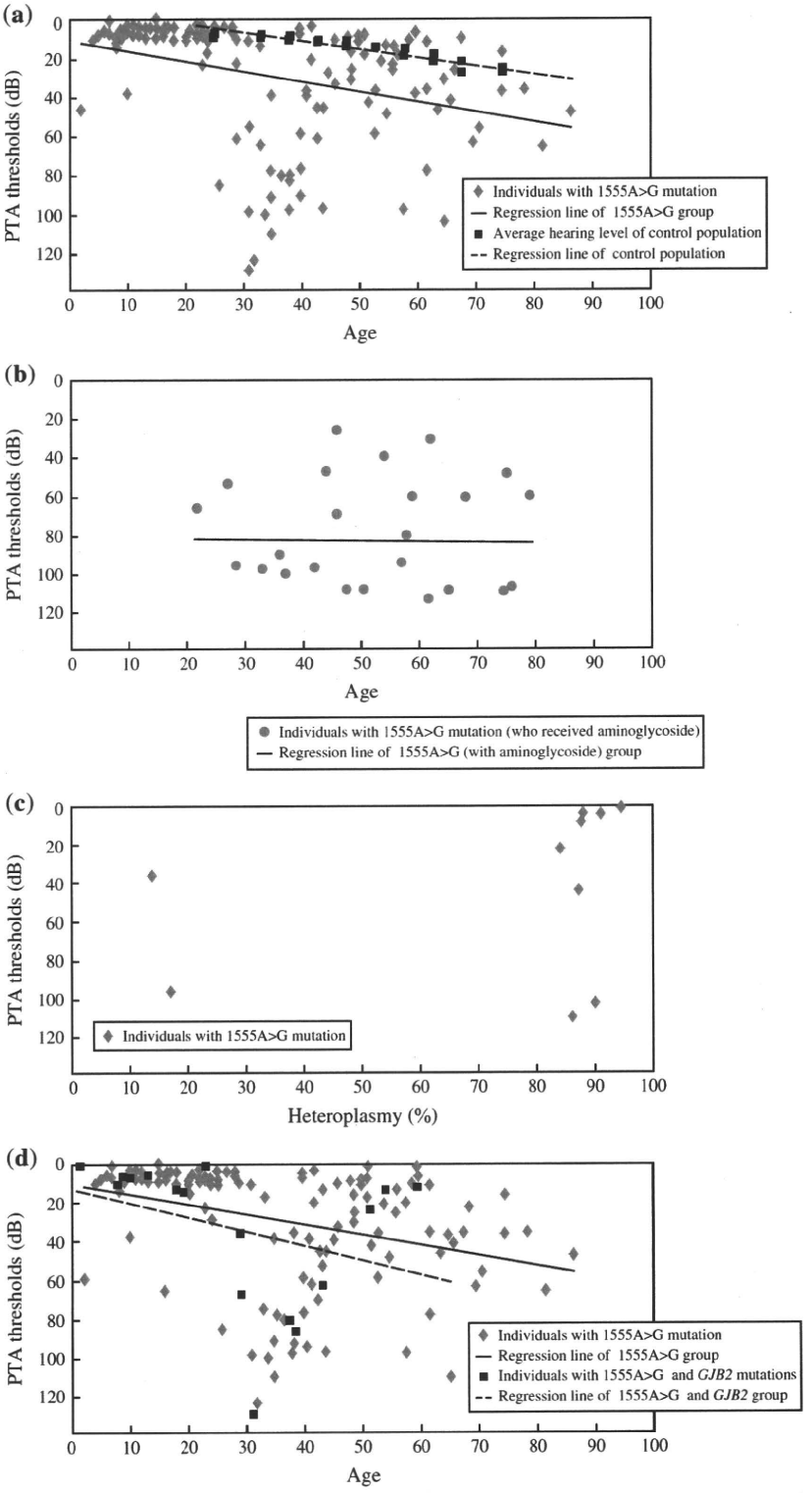

Fig. 1. Hearing levels and various parameters. **(a)** Correlation with age in the 1555A>G mutation group without reported aminoglycoside exposure compared with hearing levels in the normal Japanese population as described by Okamoto et al. (Pure-Tone Hearing Levels According to Age. Audiology Japan 1989: 32:82: 81–86, in Japanese). **(b)** Correlation with age in individuals with the 1555A>G mutation who reported aminoglycoside exposure. **(c)** Correlation with heteroplasmy in individuals with the 1555A>G mutation and no reported aminoglycoside exposure. **(d)** Comparison with age in individuals with the 1555A>G mutation with and without *GJB2* mutations but with no reported aminoglycoside exposure.

suggests that the 1555A>G mitochondria mutation itself or a modifier gene may play a role in aggravating hearing loss. Hearing of the individuals with the 1555A>G mutation also worsened with age; however, the progression speed did not differ from that found in the normal population (Fig. 1a). Interestingly, most of the worst pure-tone audiometry thresholds were clustered in the age range of 30–50 years, indicating possible unreported aminoglycoside exposure as their childhoods coincided with the period in which aminoglycosides were most commonly used in

Table 1. Allele frequency of *GJB2* mutations in 1555A>G and control groups

GJB2 mutations (all hetero genotype)	Mitochondria 1555A>G (n = 26, 14 families)		Control (n = 252)	
	Family number[a]	Allele frequency (%)	Family number	Allele frequency (%)
V37I	2.85	2.13	3	0.60
G45E/Y136X	1.94	1.45	0	0.00
235 del C	1.45	1.08	2	0.40
176-191 del 16bp	0.5	0.37	0	0.00
299-300 del AT	0.19	0.14	0	0.00
Y136H	1	0.75	2	0.40
Total	7.93	5.92	7	1.40

[a]Family numbers in the 1555A>G group were calculated by the following formula: number of family members with the 1555A>G and *GJB2* mutations divided by the total number of family members.

clinical practice including for treatment of childhood infections (1960s to 1980s). Given the above, worsened hearing and mitochondrial function may be related to genetic background (the 1555A>G mitochondrial mutation itself or modifier genes), rather than environmental factors such as noise, because older persons would be expected to have had more exposure to various environmental events and therefore to have a steeper progressive curve.

One significant factor that determines the expression of mitochondrial disease is heteroplasmy. In this study, we confirmed that heteroplasmy existed in about 5% of the subjects with the 1555A>G mutation. The mitochondrial 1555A>G mutation had been thought to transmit only in a homoplasmic state, but recently, heteroplasmic cases have been found to exist and furthermore to be associated with severe hearing loss (9). Analysis of genotype–phenotype correlation indicated that subjects carrying less than 20% of mutant copies were asymptomatic or had a mild hearing loss (9). However, such correlation was not observed in our sample. It should be noted that it is difficult to determine the correlation of heteroplasmy levels with severity of hearing loss because the mutation load in blood may be different from that occurring in the inner ear.

The group that had reported aminoglycoside exposure had moderate-to-severe hearing impairment regardless of age, confirming that aminoglycoside exposure is the most important environmental factor affecting the phenotypic expression of the 1555A>G mitochondrial mutation.

A series of studies indicated that the nuclear background might be involved in modulating the phenotypic expression of the 1555A>G mitochondrial mutation (11). Genome-wide research has suggested that a region in chromosome 8p23.1 is a candidate region as a modifier gene for phenotypic expression (12). Efforts have been made by genotyping and linkage analysis to find nuclear genes that interact with the 1555A>G mutation to cause hearing loss, but no such single gene has yet been identified. Recently, mutations in TRMU were shown to modify the phenotype of the patients with the 1555A>G mutation (14). According to Guan et al., homozygous mutation in this gene leads to a marked failure in mitochondrial tRNA metabolisms, causing impaired mitochondrial protein synthesis.

We previously reported a high prevalence of *GJB2* heterozygous mutations in patients bearing the 1555A>G mitochondrial mutation and described a family in which potential interaction between *GJB2* and a mitochondrial gene appears to be the cause of hearing impairment (13). In that family, patients who are heterozygotes for the *GJB2* mutant allele showed hearing loss more severe than that seen in siblings lacking a mutant *GJB2* allele, suggesting that heterozygous *GJB2* mutations may synergistically cause hearing loss in the presence of a 1555A>G mutation. This indicates that *GJB2* mutations may sometimes be an aggravating factor in addition to aminoglycosides in the phenotypic expression in the non-syndromic hearing loss associated with the 1555A>G mitochondrial mutation (13). Our updated results in this study revealed that 5.92% of the alleles harbored the *GJB2* mutation, and this frequency is significantly (approximately) fourfold higher than that in the normal population, in line with our previous data. However, on average, in the patients without reported aminoglycoside exposure, the hearing loss severity in the 21 individuals with the *GJB2* mutation tended to be worse but not statistically significant when compared with the 165 individuals without the *GJB2* mutation.

Alternatively, it may merely be due to assortative mating having caused accelerated accumulation of various genes in one family (16).

Further study is needed to elucidate the interaction between the *GJB2* mutations and the 1555A>G mutation.

Acknowledgements

The authors are grateful to the patients and families who participated in this study and to A. C. Apple-Mathews for assistance in preparing the manuscript. This study was supported by a Health Sciences Research Grant (Research on Eye and Ear Science, Immunology, Allergy and Organ Transplantation) from the Ministry of Health and Welfare of Japan and by the Acute Profound Deafness Research Committee of the Ministry of Health and Welfare of Japan.

References

1. Usami S, Abe S, Akita J et al. Prevalence of mitochondrial gene mutations among hearing impaired patients. J Med Genet 2000a: 37: 38–40.
2. Prezant T, Agapian J, Bohlman M et al. Mitochondrial ribosomal RNA mutation associated with both antibiotics-induced and non-syndromic deafness. Nat Genet 1993: 4: 289–294.
3. Hutchin T, Haworth J, Higashi K. A molecular basis for human hypersensitivity to aminoglycoside antibiotics. Nucleic Acids Res 1993: 21: 4174–4179.
4. Usami S, Abe S, Kasai M et al. Genetic and clinical features of sensorineural hearing loss associated with the 1555A>G mitochondrial mutation. Laryngoscope 1997: 107: 483–490.
5. Estivill X, Govea N, Barceló E et al. Familial progressive sensorineural deafness is mainly due to the mtDNA A1555G mutation and is enhanced by treatment with aminoglycosides. Am J Hum Genet 1998: 62: 27–35.
6. Usami S, Abe S, Akita J et al. Sensorineural hearing loss associated with the mitochondrial mutations. Adv Otorhinolaryngol 2000b: 56: 203–211.
7. Noguchi Y, Yashima T, Ito T et al. Audiovestibular findings in patients with mitochondrial A1555G mutation. Laryngoscope 2004: 114 (2): 344–348.
8. Abe S, Yamaguchi T, Usami S. Application of deafness diagnostic screening panel based on deafness mutation/gene database using invader assay. Genet Test 2007: 11: 333–340.
9. del Castillo FJ, Rodriguez-Ballesteros M, Martin Y et al. Heteroplasmy for the 1555A>G mutation in the mitochondrial 12S rRNA gene in six Spanish families with non-syndromic hearing loss. J Med Genet 2003: 40 (8): 632–636.
10. Usami S, Abe S, Shinkawa H et al. Rapid mass screening method and counseling for the 1555A>G mitochondrial mutation. J Hum Genet 1999: 44 (5): 304–307.
11. Bykhovskaya Y, Shohat M, Ehrenman K et al. Evidence for complex nuclear inheritance in a pedigree with non-syndromic deafness due to a homoplasmic mitochondrial mutation. Am J Med Genet 1998: 77 (5): 421–426.
12. Bykhovskaya Y, Estivill X, Taylor K et al. Candidate locus for a nuclear modifier gene for maternally inherited deafness. Am J Hum Genet 2000: 66: 1905–1910.
13. Abe S, Kelley PM, Kimberling WJ et al. Connexin 26 gene (GJB2) mutation modulates the severity of hearing loss associated with the 1555A>G mitochondrial mutation. Am J Med Genet 2001: 103 (4): 334–338.
14. Guan MX, Yan Q, Li X et al. Mutation in TRMU related to transfer RNA modification modulates the phenotypic expression of the deafness-associated mitochondrial 12S ribosomal RNA mutations. Am J Hum Genet 2006: 79: 291–302.
15. Abe S, Usami S, Shinkawa H et al. Prevalent connexin 26 gene (GJB2) mutations in Japanese. J Med Genet 2000: 37 (1): 41–43.
16. Nance WE, Kearsey MJ. Relevance of connexin deafness (DFNB1) to human evolution (Review). Am J Hum Genet 2004: 74: 1081–1087.

Neuroscience 154 (2008) 22–28

THE LOCALIZATION OF PROTEINS ENCODED BY *CRYM*, *KIAA1199*, *UBA52*, *COL9A3*, AND *COL9A1*, GENES HIGHLY EXPRESSED IN THE COCHLEA

S. USAMI,[a]* Y. TAKUMI,[a] N. SUZUKI,[a] T. OGUCHI,[a] A. OSHIMA,[a] H. SUZUKI,[a] R. KITOH,[a] S. ABE,[b] A. SASAKI[c] AND A. MATSUBARA[c]

[a]*Department of Otorhinolaryngology, Shinshu University School of Medicine, 3-1-1 Asahi, Matsumoto 390-8621, Japan*

[b]*Division of Advanced Technology and Development, BML, Inc., 1361-1 Matoba, Kawagoe-shi, Saitama 350-1101, Japan*

[c]*Department of Otorhinolaryngology, Hirosaki University Graduate School of Medicine, 5 Zaifu-cho, Hirosaki 036-8562, Japan*

Abstract—Genes that are highly expressed in the inner ear, as revealed by cDNA microarray analysis, may have a crucial functional role there. Those that are expressed specifically in auditory tissues are likely to be good candidates to screen for genetic alterations in patients with deafness, and several genes have been successfully identified as responsible for hereditary hearing loss. To understand the detailed mechanisms of the hearing loss caused by the mutations in these genes, the present study examined the immunocytochemical localization of the proteins encoded by *Crym*, *KIAA1199 homolog*, *Uba52*, *Col9a3*, and *Col9a1* in the cochlea of rats and mice. Confocal microscopic immunocytochemistry was performed on cryostat sections. Ultrastructurally, postembedding immunogold cytochemistry was applied using Lowicryl sections. Crym protein was predominantly distributed in the fibrocytes in the spiral ligament, as well as the stria vascularis in rats. KIAA1199 protein homolog was localized in various supporting cells, including inner phalangeal, border, inner and outer pillar, and Deiters' cells. Uba52 protein was restrictedly localized within the surface of the marginal cells of the stria vascularis. Collagen type IX was found within the tectorial membrane as well as fibrocytes in the spiral ligament. The present results showed cell-specific localization of the encoded proteins of these highly expressed genes, indicating that the coordinated actions of various molecules distributed in different parts of the cochlea are essential for maintenance of auditory processing in the cochlea.

Key words: *CRYM*, *KIAA1199*, *UBA52*, *COL9A3*, *COL9A1* cochlea.

The coordinated actions of various molecules are essential for the normal development and maintenance of auditory processing in the cochlea. Thorough analysis of gene expression profiles in human inner ear tissues using a cDNA microarray containing 23,040 genes identified 52 highly expressed genes whose signal intensities were more than 10-fold higher in the cochlea and vestibule than in a mixture of 29 other tissues (Abe et al., 2003a). These genes may have a crucial functional role in the inner ear, therefore, genes with unique function and specific expression in the cochlea are excellent candidates as causative genes of human non-syndromic deafness. Among those genes, we have focused on five, *CRYM*, *KIAA1199*, *UBA52*, *COL9A3* and *COL9A1*, because of their high expression ratio in the cochlea compared with other tissues (119.55, 56.54, 37.41, 17.64, 11.88 respectively) and subsequent mutation screening has detected possible disease causing mutations in some of them.

The *CRYM* gene shows the second highest expression in the human cochlea, after *COCH*, and a search for mutations of *CRYM* among non-syndromic deafness patients identified two mutations found at the C-terminus (Abe et al., 2003a). CRYM protein (crystallin, mu) is known to be identical to T3 (triiodothyronine) -binding protein and it binds to T3 in the presence of nicotinamide adenine dinucleotide phosphate (NADPH), and might retain the intracellular free T3 concentration (Suzuki et al., 2007 for review). Our recent study demonstrated that one mutant has no binding capacity to T3, implicating that *CRYM* mutations cause auditory dysfunction through thyroid hormone binding properties (Oshima et al., 2006). Although thyroid hormone is known to be crucial for normal development as well as maintenance of hearing function, the detailed mechanism of thyroid hormone handling in the inner ear has not been well understood.

The gene encoding *KIAA1199* showed a high level of expression in the inner ear by complementary DNA (cDNA) microarray analysis (Abe et al., 2003a). Previous *in situ* hybridization findings suggested that *KIAA1199* is expressed in Deiters' cells and/or the spiral ligament, and subsequent mutation screening identified mutations in non-syndromic hearing loss patients with high-frequency predominant hearing loss (Abe et al., 2003b). Despite the abundant expression in the inner ear, the precise localization as well as detailed function is not yet known.

Uba52 is a 128-amino acid fusion protein consisting of a 52-amino acid tail fused to a 76-amino acid ubiquitin peptide. The 52-amino acid tail is a ubiquitin carboxyl extension protein and is a component of ribosome that is removed from ubiquitin before maturation of the ribosome. Ubiquitin is a highly conserved protein that plays, through the so-called ubiquitin–proteasome pathway, a fundamental role in mediating intracellular selective protein degradation. In this pathway, ubiquitin molecules attach to protein substrates by a multienzymatic pathway and ubiquiti-

*Corresponding author. Tel: +81-263-37-2666; fax: +81-263-36-9164.
E-mail address: usami@hsp.md.shinshu-u.ac.jp (S. Usami).
Abbreviations: cDNA, complementary DNA; HAS, human serum albumin; TBST, Tris-buffered saline containing 0.1% Triton X-100.

0306-4522/08$32.00+0.00
doi:10.1016/j.neuroscience.2008.03.018

nated substrates are degraded by proteasome (Schwartz and Ciechanover, 1999 for review). Although they are highly expressed in the inner ear, the functional significance and relevance to disorders of ubiquitin in the inner ear are still unknown.

Collagen type IX is a heterotrimer of three genetically different alpha chains, alpha I (IX), alpha II (IX), and alpha III (IX). Because cDNA microarray analysis has shown *COL9A1* and *COL9A3* to be highly expressed in the human inner ear (Abe et al., 2003a), type IX collagen, a member of the FACIT (Fibril-Associated Collagen with Interrupted Triplet helices) group of collagens that bind to the surface of fibril-forming type II collagen, may play an important role in the inner ear, type IX collagen, as well as type II and V collagens, also is an important component in the tectorial membrane of the organ of Corti (Slepecky et al., 1992a,b). The non-syndromic hearing loss patients with the *COL9A3* mutations showed a moderate progressive bilateral sensorineural hearing impairment in all frequencies (Asamura et al., 2005a). We also identified a *COL9A1* mutation in a family showing symptoms characteristic of Stickler syndrome, including moderate-to-severe sensorineural hearing loss, moderate-to-high myopia with vitreoretinopathy, and epiphyseal dysplasia (Van Camp et al., 2006).

A series of these studies suggested that these five molecules might have crucial functions with regard to hearing. As the first step toward complete understanding of the detailed function of these molecules in the cochlea, the present study reviewed the current knowledge of these genes and examined the cellular and sub-cellular localization of the proteins encoded by *Crym*, *KIAA1199 homolog*, *Uba52*, *Col9a3*, and *Col9a1* in the cochlea of rats and mice.

EXPERIMENTAL PROCEDURES

Tissue preparation

Wistar rats and C57BL/6J mice (CLEA Japan, Inc., Tokyo, Japan) were used in the present study. The animals were deeply anesthetized with sodium pentobarbital (50 mg/kg). For the confocal microscopic analysis, 1 ml of fixative (4% formaldehyde in 0.1 M phosphate buffer, pH 7.25) was injected through the tympanic membrane and for the electron microscopical analysis perilymphatic perfusion was performed by injection of 1 ml of fixative (4% formaldehyde and 0.5% glutaraldehyde) into the scala tympani. Subsequently, the animals were perfused through the heart by the same fixative used for tympanic injection or perilymphatic perfusion. Then the temporal bones were removed and postfixed in the same fixative (4–8 h, 4 °C). For confocal microscopy analysis, the specimens were immersed in 10% sucrose and 30% sucrose (each overnight) and then serial cryostat sections (15 μm thick) were cut and placed on silane-coated slides. For electron microscopy, the specimens were cryo-protected, quick frozen, freeze-substituted, and low temperature embedded in a methacrylate resin (Lowicryl HM 20; Chemische Werke Lowi, Waldkraiburg, Germany).

Polyclonal antibodies

Preparation of polyclonal antibodies to Crym protein, KIAA1199 protein homolog, and Uba52 protein were as follows. Sequences were chosen from mouse Crym protein (AFLSAEEVQDHLRSC and EGHSNTAVPSHQASC), mouse Uba52 protein (VKAKIQDKEGIP-PDC and RKKKCGHTNNLRPKK), and mouse KIAA1199 protein homolog (YRSKKESERLVQYLC and NDFAYIEVDGRRYPC), to synthesize peptides. The peptides, coupled to keyhole limpet hemocyanin (KLH), were mixed with complete adjuvant and injected into rabbits (Crym protein, KIAA1199 protein homolog) or guinea pigs (Uba52 protein). The antiserum was affinity purified on a column carrying the peptide used for immunization. Antibodies against collagen type IX (COSMO BIO Co., Ltd., Tokyo, Japan or Calbiochem, San Diego, CA, USA), von Willebrand factor (to detect alpha-tectorin) (Chemicon, Temecula, CA, USA), and GST7-7(P) (kindly provided by Dr. Shigeki Tsuchida, Hirosaki University) were also used.

Immunocytochemistry

The tissue specimens were incubated as follows: (1) normal goat serum at room temperature for 30 min, (2) rabbit polyclonal antibodies Crym protein, KIAA1199 protein homolog, collagen type IX, GST7-7(P) (1:10,000, 1:250, 1:200 dilution respectively), or guinea-pig polyclonal anti-Uba52 protein antibody (1:200 dilution) diluted with 0.3% Triton X-100, overnight at 4 °C, (3) Rhodamine-conjugated anti-rabbit antibodies (Chemicon; 1:150 dilution for Crym protein, KIAA1199 protein homolog, collagen type IX, GST7-7(P)), or FITC conjugated goat anti-guinea-pig antibodies (MP Biomedicals, Irvine, CA, USA; 1:150 dilution for Uba52 protein), 4 h at room temperature. The specimens were examined with a confocal laser scanning microscope (Leica TCS SP2 ABOS). For control, adsorption experiments were carried out by blocking with the synthetic peptides. Specificity of the antisera was also examined by immunoblotting analysis (Oshima et al., 2006; Kitoh et al., 2007).

Postembedding immunogold staining of ultrathin sections

Ultrathin sections were briefly (2–3 s) immersed in a saturated solution of NaOH in absolute ethanol, rinsed well with double-distilled water, and incubated in the following solutions (at room temperature): (1) 0.1% sodium borohydride and 50 mM glycine in Tris-buffered saline containing 0.1% Triton X-100 (TBST) (10 min), (2) 2% human serum albumin (HSA) in TBST (10 min), (3) primary antibodies (1:10,000 for Crym protein, 1:200 for Uba52 protein, 1:250 for KIAA1199 protein homolog, 1:200 for collagen type IX, 1:100 for von Willebrand factor) in TBST containing 2% HSA (2 h), (4) 2% HSA in TBST (10 min), and (5) secondary 15 nm gold-coupled goat anti-rabbit IgG (AuroProbe EM GAR15, GE Healthcare, Buckinghamshire, UK), or 18 nm gold-coupled anti-guinea-pig IgG (Jackson ImmunoResearch Laboratories, Inc., West Grove, PA, USA) diluted 1:20 in TBST containing 2% HSA and polyethylene glycol (5 mg/ml, 2 h). The sections were rinsed well between steps (3)-(5), counterstained by uranyl acetate and lead citrate, and examined in a JEOL 1200CX electron microscope.

All studies were carried out in accordance with Fundamental Guidelines for Proper Conduct of Animal Experiment and Related Activities in Academic Research Institutions under the jurisdiction of the Ministry of Education, Culture, Sports, Science and Technology, Japan. Every effort was made to minimize the number of animals used and their suffering.

RESULTS

Crym protein was localized in type II fibrocytes of the spiral ligament in the cochlea in mice and rats (Fig. 1A). In rats, it was also distributed in the stria vascularis (Fig. 1B). Ultrastructurally, Crym protein was localized in the nucleus

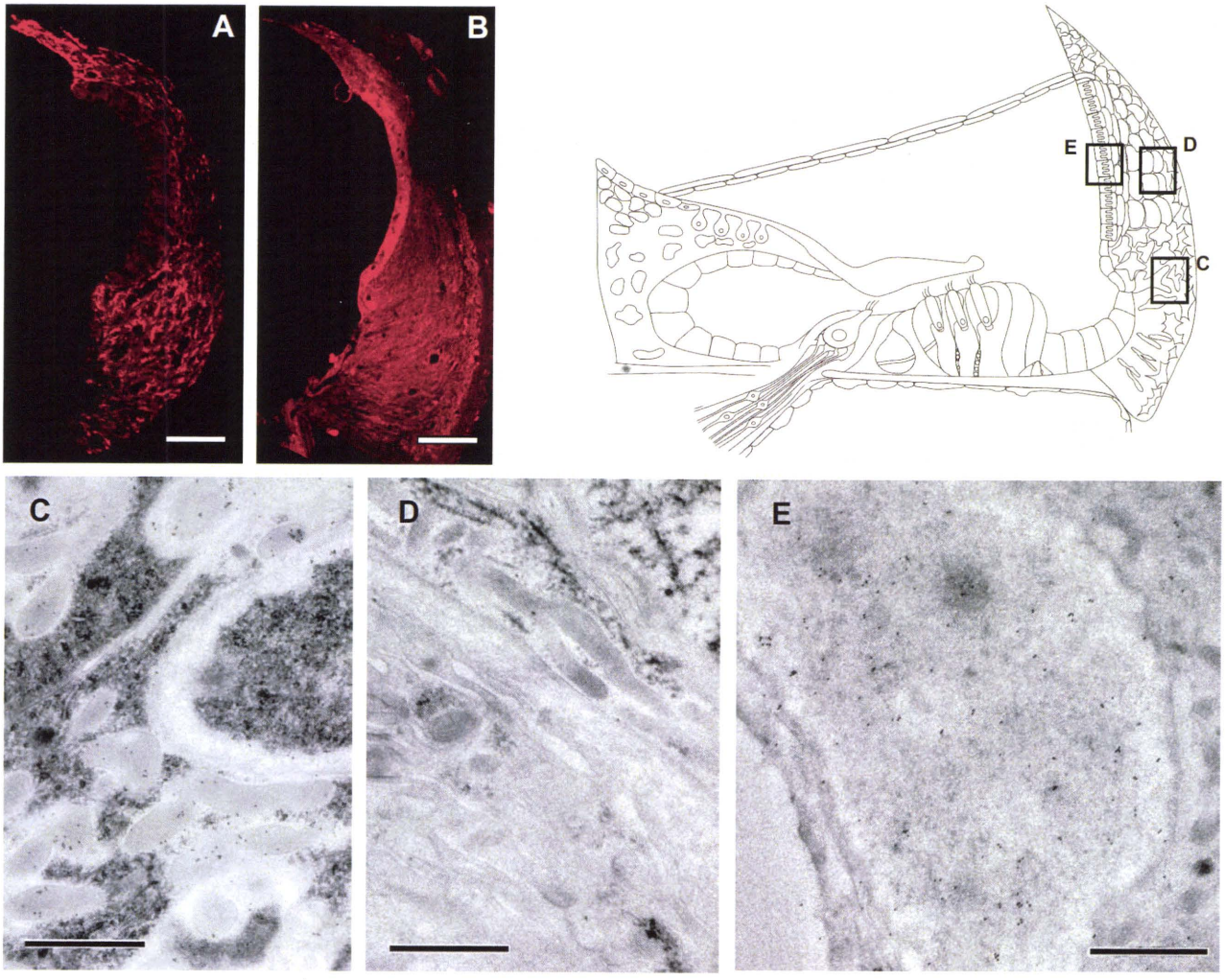

Fig. 1. Immunocytochemical localization of Crym protein in mice (A) and rats (B). Crym protein is distributed in type II fibrocytes of the spiral ligament in the cochlea in mice and rats. In the rat, Crym protein is also distributed in the stria vascularis. Immuno-electron micrograph showing Crym protein localized in the nucleus and mitochondria in type II fibrocytes (C) and marginal cells (E). No immunoreactivity is found in type I fibrocytes (D). Scale bars=50 μm (A, B), 1 μm (C–E).

and mitochondria in type II fibrocytes and marginal cells (Fig. 1C, E). Type I fibrocytes neighboring type II fibrocytes were devoid of immunoreactivity (Fig. 1D).

KIAA1199 protein homolog was distributed in the Deiters' cells, as well as various supporting cells in the organ of Corti including border, inner phalangeal, and inner and outer pillar cells (Fig. 2A). Mice and rats showed similar distribution. Electron microscopically, KIAA1199 protein homolog was evenly distributed in the cytoplasm of various supporting cells (Fig. 2B).

Uba52-immunoreactivities were observed in the marginal cells of the stria vascularis in rats as well as mice (Fig. 3A). No staining was shown in the intermediate and basal cells, being confirmed by double staining with GST7-7(P) which is a known marker for intermediate cells in the stria vascularis (Fig. 3A) (Takumi et al., 2001). At the ultrastructural level, labeled gold particles were evenly distributed in cytoplasm and nucleus of the marginal cells (Fig. 3B).

Type IX collagen-immunoreactivity was predominantly distributed in the tectorial membrane (Fig. 4A). At the electron microscopic level, gold particles were localized within the radial collagen fibril bundles which have a cross-striated pattern coursed in a parallel and well-organized manner among a laminated, striated-sheet matrix, where collagen type IX immunoreactive gold particles were not found (Fig. 4B). In contrast, gold particles indicating alpha-tectorin were distributed in a laminated, striated-sheet matrix area (Fig. 4C). Weak immunoreactivity was also found in the spiral limbus and the spiral ligament in mice and rats (Fig. 4A). In the type II fibrocytes, collagen type IX immunoreactive gold particles were associated with the collagen fibers (Fig. 4D).

For all antibodies, no significant staining was observed in the control sections (data not shown).

DISCUSSION

Highly expressed genes in the inner ear, determined by cDNA microarray analysis (Abe et al., 2003a), may have crucial functional roles in the cochlea and are therefore likely to be good candidates to screen for genetic alter-

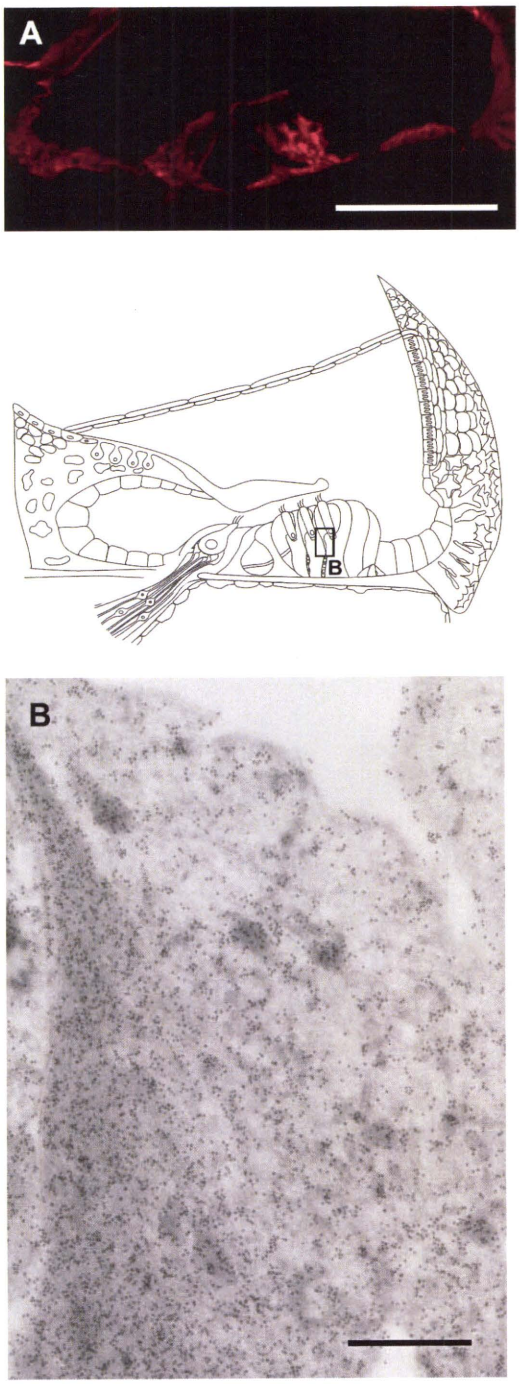

Fig. 2. Immunocytochemical localization of KIAA1199 protein homolog in rats. KIAA1199 protein homolog is distributed in the Deiters' cells, as well as various supporting cells in the organ of Corti including border, inner phalangeal, and inner and outer pillar cells (A). An immuno-electron micrograph showing KIAA1199 protein evenly distributed in the cytoplasm of Deiters' cells (B). Scale bars=100 μm (A), 1 μm (B).

ations in patients with deafness. Our series of screening studies demonstrated these genes are responsible for hearing loss in patients (Abe et al., 2003a,b; Asamura et al., 2005a; Van Camp et al., 2006). In this study, by means of immunocytochemical approach, we demonstrated detailed localization of proteins encoded by *Crym*, *KIAA1199*, *UbA52*, *Col9a3*, and *Col9a1*, at both the light microscopic and electron microscopic levels.

Crym protein is distributed in the spiral ligament and stria vascularis

Regarding the sites in the cochlea where *CRYM* acts, it has been shown to be distributed in the spiral ligament by *in situ* hybridization (Abe et al., 2003a) and confirmed by immunocytochemical methods in the type II fibrocytes of the spiral ligament (Oshima et al., 2006). The present study further confirmed the sites within the cochlea where *Crym* is functioning, i.e. type II fibrocytes in the spiral ligament in mice, and in rats where it was also distributed in the stria vascularis. From such immunocytochemical findings, we speculated that *Crym* might be involved in the potassium-ion recycling system via Na,K-ATPase because: 1) Na,K-ATPase is enriched in type II fibrocytes, 2) a functional T3 response element was identified in the promoter region of the Na,K-ATPase β1 gene, 3) Na,K-ATPase activity was stimulated by T3 in various tissues, and 4) the two molecules are likely to be co-localized in type II fibrocytes (for references, see discussion in Oshima et al., 2006).

With regard to the subcellular localization of the T3 binding site, the endoplasmic reticulum, mitochondria, nuclear envelope, and cytoplasm have been postulated by protein-binding analysis (Suzuki et al., 2007 for review). The present electron microscopic findings indicated that mitochondria and nucleus are possible sites where *Crym* is functioning. It is well known that the action of thyroid hormone is initiated through the activation of gene expression by binding to its nuclear receptor (Lazar, 1993). Mitochondria are also considered to be one of the candidates as a direct target for thyroid hormones (Psarra et al., 2006).

KIAA protein homolog localized in various supporting cells

The present study demonstrated KIAA1199 protein homolog in the Deiters' cells as well as other supporting cells in the organ of Corti. Although the detailed function of KIAA1199 protein is still unknown, it, and two structurally similar proteins on the basis of a BLAST search, TMEM2 and PKHD1, are known to have common protein domains named G8 containing proteins, predicted to be membrane-integrated or secreted (He et al., 2006). Using immortal renal cell carcinoma cells, a striking upregulation of *KIAA1199* mRNA in mortal cell lines compared with immortal cell lines suggested that *KIAA1199* may play a role in cellular mortality of normal human cells (Michishita et al., 2006).

Uba52 protein restrictively localized in the marginal cells of the stria vascularis

With regard to the localization of Uba52 in the inner ear, we first reported that Uba52-immunoreactivities were observed in the marginal cells of the stria vascularis in rats as well as mice (Kitoh et al., 2007). Since the stria vascularis

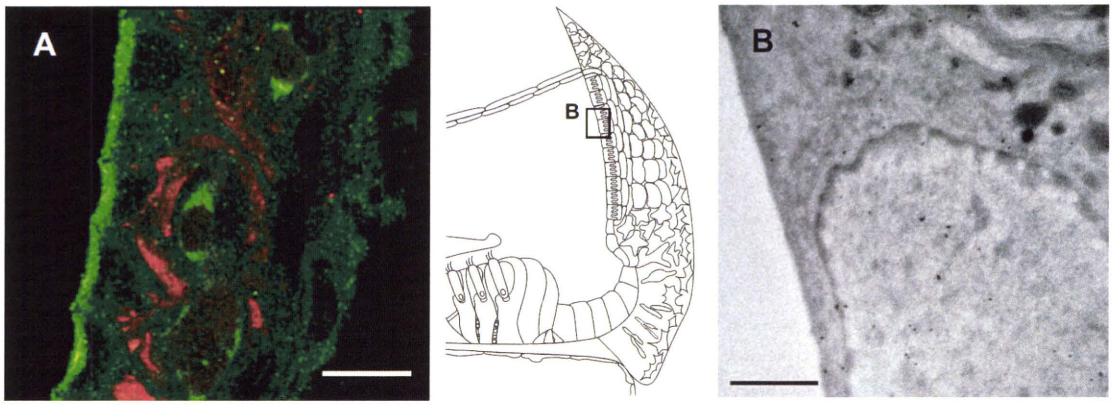

Fig. 3. Immunocytochemical localization of Uba52 protein in mice. Uba52 protein (green) is distributed in the marginal cells of the stria vascularis (A). GST7-7(P) (red) is found in intermediate cells in the stria vascularis (A). An immuno-electron micrograph showing Uba52 protein evenly distributed in cytoplasm and nucleus of the marginal cells (B). Scale bars=15 μm (A), 1 μm (B).

is known to be important for maintaining endolymphatic potassium ion concentration, Uba52 protein may have a functional role in the regulation of ion homeostasis in the inner ear. Our recent developmental study indicated that Uba52 immunoreactivity is correlated with the morphological maturation and increase of endolymph K^+ concentration, suggesting that the Uba52 proteins are possibly relevant to the function of the strial marginal cells, for example in K^+ recycling (Kitoh et al., 2007). We also performed mutation screening for UBA52 in 160 non-syndromic deafness patients, but no mutations were identified (Kitoh et al., 2007). This may not mean that ubiquitin is not necessary to maintain normal hearing function, in fact most of the ubiquitin-related diseases are induced by abnormalities of the substrates of the ubiquitin or enzymes in the pathway (Schwartz and Ciechanover, 1999 for review). The proteins of ubiquitination targets or enzymes in the inner ear are not known, but new pathological models of inner ear

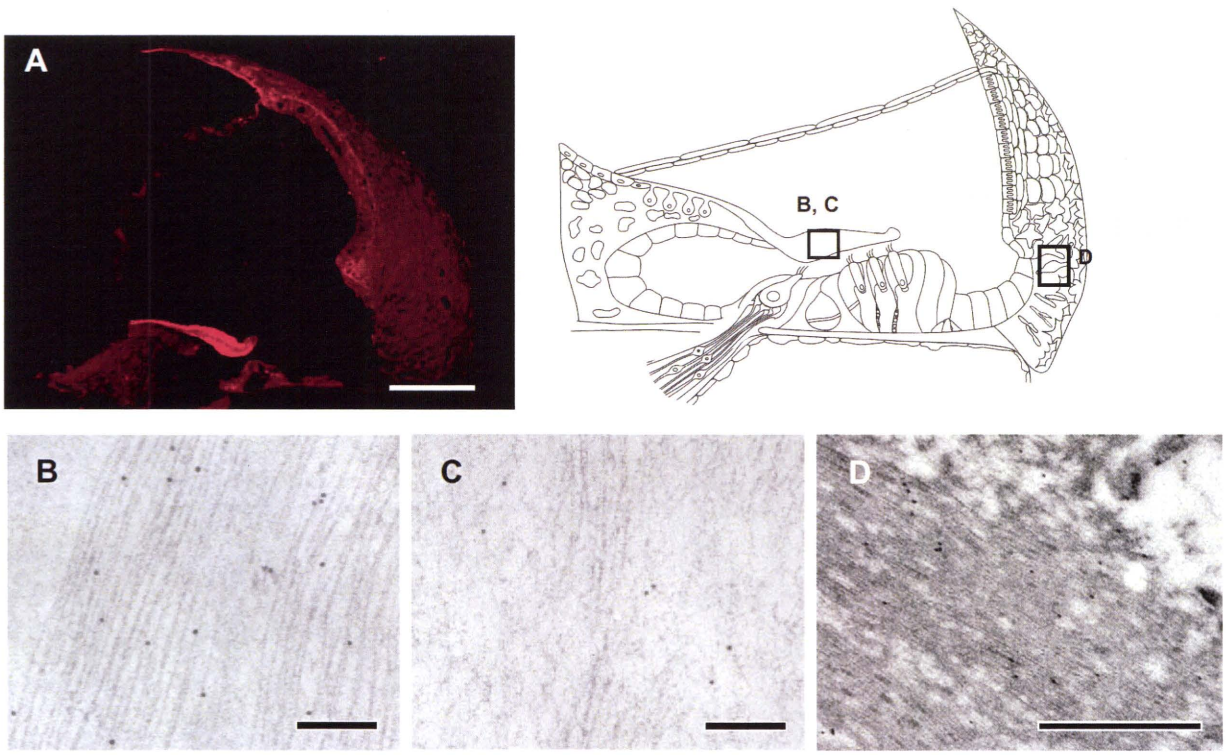

Fig. 4. Type IX collagen-immunoreactivity is predominantly distributed in the tectorial membrane of the rat cochlea (A). Weak immunoreactivity is also found in the spiral limbus and the spiral ligament (A). At the electron microscopic level, gold particles are localized within the radial collagen fibril bundles (B), which have a cross-striated pattern coursed in a parallel and well-organized manner (B). In contrast, gold particles indicating alpha-tectorin are distributed in a laminated, striated-sheet matrix area (C). In the type II fibrocytes, collagen type IX immunoreactive gold particles are associated with the collagen fibers (D). Scale bars=100 μm (A), 200 nm (B–D).

disorders may be found by further study. We are currently searching for candidate proteins by proteomic analysis using two-dimensional gel electrophoresis, and have found several candidates (Kitoh et al., manuscript in preparation). Hearing loss induced by ubiquitin will be a challenging research field for the near future.

Collagen type IX is localized in the tectorial membrane, limbs, and spiral ligament

Collagen in the inner ear is of great interest because mutations of several types of collagen have been reported to be responsible for syndromic as well as non-syndromic hearing loss (see Hereditary Hearing Loss Homepage: http://www.uia.ac.be/dnalab/hhh/).

The present results replicated our previous immunocytochemical data, in which type IX collagen is distributed in the tectorial membrane, where it co-localizes with type II collagen suggesting that type IX collagen contributes to the three-dimensional integrated structure of type II collagen molecules (Asamura et al., 2005b). Type IX collagen likely plays an important role in the maintenance of normal hearing as shown by assessment by auditory brain stem response in mice with targeted disruption of the *col9a1* gene. The tectorial membrane of knockout mice was shown to be abnormal in shape by light microscopy, and electron microscopy revealed disturbance of the organization of the collagen fibrils. Type II collagen immunoreactivity in the tectorial membrane of type IX collagen knockout mice was not found, therefore, it is likely that a lack of type IX collagen affects the three-dimensional structure of type II collagen molecules (Suzuki et al., 2005). The above suggest that in the auditory system, genes encoding each chain of type IX collagen fulfill important functions associated with the tectorial membrane. The present immunoelectron microscopic findings not only confirmed the light microscopic observation, but also revealed the detailed localization patterns within the tectorial membrane. The tectorial membrane is known to be composed of two morphologically different areas (Goodyear and Richardson, 2002), and type IX immunolabeling was associated with radial collagen fibril bundles in the striated-sheet matrix area. The latter area is immunolabeled with alpha-tectorin, which is also known to be one of the important components in the extracellular matrix in the tectorial membrane (Verhoeven et al., 1998). There is an absence of cross-striated patterns in the radial collagen fibril bundles and aggregated/fused fibrils in homozygous knockout mice (Suzuki et al., 2005), indicating that type IX collagen is essential for intact three dimensional structure in association with type II collagen or other molecules.

CONCLUSION

The present immunocytochemical study confirmed the cell-specific localization of the encoded proteins of highly expressed genes in the inner ear. These proteins may have a crucial functional role in the inner ear, and dysfunction of these proteins may lead to hearing disturbance with various clinical symptoms. Future functional as well as mutation screening studies will be crucial to understanding the mechanisms of hearing.

Acknowledgments—We are sincerely grateful to Kirsten K. Osen for introducing us to an attractive scientific field. We hope that this study will contribute information toward understanding hearing function and therapy of hearing loss. We also thank Mr. Shinya Nishio and A. C. Apple-Mathews for help in preparing the manuscript. This work was supported by a Health Sciences Research Grant (Research on Eye and Ear Science, Immunology, Allergy and Organ Transplantation) from the Ministry of Health and Welfare of Japan (S.U.), the Acute Profound Deafness Research Committee of the Ministry of Health and Welfare of Japan (S.U.), and a Grant-in-Aid for Scientific Research from the Ministry of Education, Science and Culture of Japan (S.U.).

REFERENCES

Abe S, Katagiri T, Saito-Hisaminato A, Usami S, Inoue Y, Tsunoda T, Nakamura Y (2003a) Identification of CRYM as a candidate responsible for nonsyndromic deafness, through cDNA microarray analysis of human cochlear and vestibular tissues. Am J Hum Genet 72:73–82.

Abe S, Usami S, Nakamura Y (2003b) Mutations in the gene encoding KIAA1199 protein, an inner-ear protein expressed in Deiters' cells and the fibrocytes, as the cause of nonsyndromic hearing loss. J Hum Genet 48:564–570.

Asamura K, Abe S, Imamura Y, Aszodi A, Suzuki N, Hashimoto S, Takumi Y, Hayashi T, Fassler R, Nakamura Y, Usami S (2005b) Type IX collagen is crucial for normal hearing. Neuroscience 132:493–500.

Asamura K, Abe S, Fukuoka H, Nakamura Y, Usami S (2005a) Mutation analysis of COL9A3, a gene highly expressed in the cochlea, in hearing loss patients. Auris Nasus Larynx 32:113–117.

Goodyear RJ, Richardson GP (2002) Extracellular matrices associated with the apical surfaces of sensory epithelia in the inner ear: molecular and structural diversity. J Neurobiol 53:212–227.

He QY, Liu XH, Li Q, Studholme DJ, Li XW, Liang SP (2006) G8: a novel domain associated with polycystic kidney disease and nonsyndromic hearing loss. Bioinformatics 22:2189–2191.

Kitoh R, Oshima A, Suzuki N, Hashimoto S, Takumi Y, Usami S (2007) Immunocytochemical localization of ubiquitin A-52 protein in the mouse inner ear. Neuroreport 18:869–873.

Lazar MA (1993) Thyroid hormone receptors: multiple forms, multiple possibilities. Endocr Rev 14:184–193.

Michishita E, Garces G, Barrett JC, Horikawa I (2006) Upregulation of the KIAA1199 gene is associated with cellular mortality. Cancer Lett 239:71–77.

Oshima A, Suzuki S, Takumi Y, Hashizume K, Abe S, Usami S (2006) CRYM mutations cause deafness through thyroid hormone binding properties in the fibrocytes of the cochlea. J Med Genet 43:e25.

Psarra AM, Solakidi S, Sekeris CE (2006) The mitochondrion as a primary site of action of steroid and thyroid hormones: presence and action of steroid and thyroid hormone receptors in mitochondria of animal cells. Mol Cell Endocrinol 246:21–33.

Schwartz A, Ciechanover A (1999) The ubiquitin-proteasome pathway and pathogenesis of human diseases. Annu Rev Med 50:57–74.

Slepecky NB, Savage JE, Cefaratti LK, Yoo TJ (1992a) Electronmicroscopic localization of type II, IX, and V collagen in the organ of Corti of the gerbil. Cell Tissue Res 267:413–418.

Slepecky NB, Savage JE, Yoo TJ (1992b) Localization of type II, IX and V collagen in the inner ear. Acta Otolaryngol 112:611–617.

Suzuki N, Asamura K, Kikuchi Y, Takumi Y, Abe S, Imamura Y, Hayashi T, Aszodi A, Fassler R, Usami S (2005) Type IX collagen knock-out mouse shows progressive hearing loss. Neurosci Res 51:293–298.

Suzuki S, Mori J, Hashizume K (2007) μ-Crystallin, a NADPH-dependent T(3)-binding protein in cytosol. Trends Endocrinol Metab 18:286–289.

Takumi Y, Matsubara A, Tsuchida S, Ottersen OP, Shinkawa H, Usami S (2001) Various glutathione S-transferase isoforms in the rat cochlea. Neuroreport 12:1513–1516.

Van Camp G, Snoeckx RL, Hilgert N, van den Ende J, Fukuoka H, Wagatsuma M, Suzuki H, Smets RM, Vanhoenacker F, Declau F, Van de Heyning P, Usami S (2006) A new autosomal recessive form of Stickler syndrome is caused by a mutation in the COL9A1 gene. Am J Hum Genet 79:449–457.

Verhoeven K, Van Laer L, Kirschhofer K, Legan PK, Hughes DC, Schatteman I, Verstreken M, Van Hauwe P, Coucke P, Chen A, Smith RJ, Somers T, Offeciers FE, Van de Heyning P, Richardson GP, Wachtler F, Kimberling WJ, Willems PJ, Govaerts PJ, Van Camp G (1998) Mutations in the human alpha-tectorin gene cause autosomal dominant non-syndromic hearing impairment. Nat Genet 19:60–62.

(Accepted 11 March 2008)
(Available online 19 March 2008)

HUMAN MUTATION Mutation in Brief #1008, 29:E37-E46, 2008 (Online)

MUTATION IN BRIEF

Mutation Profile of the *CDH23* Gene in 56 Probands with Usher Syndrome Type I

A. Oshima[1,3], T. Jaijo[2], E. Aller[2], J.M. Millan[2], C. Carney[1], S. Usami[3], C. Moller[4], and W.J. Kimberling[1,5]

[1] *Center for the Study and Treatment of Usher Syndrome, Boys Town National research hospital, Omaha, Nebraska*

[2] *Unidad de Genetica, Hospital La Fe, Valencia Spain*

[3] *Department of Otorhinolaryngology, Shinshu University school of Medicine, Matsumoto Japan*

[4] *Department Audiology, The Swedish Institute for Disability Research, Orebro, Sweden*

[5] *Department of Ophthalmology, University of Iowa Medical School, Iowa City, Iowa.*

*Correspondence to William J. Kimberling, Center for the Study and Treatment of Usher Syndrome, Boys Town National Research Hospital, Omaha, NE 68131.

Contract grant sponsor: Foundation Fighting Blindness (BR-GE-0606-0343), National Institute of Deafness and other Communication Disorders (P01 DC01813) and in Spain by F.I.S. PI04/0918

Communicated by Mark H. Paalman

Mutations in the human gene encoding cadherin23 (*CDH23*) cause Usher syndrome type 1D (*USH1D*) and nonsyndromic hearing loss. Individuals with Usher syndrome type I have profound congenital deafness, vestibular areflexia and usually begin to exhibit signs of RP in early adolescence. In the present study, we carried out the mutation analysis in all 69 exons of the *CDH23* gene in 56 Usher type 1 probands already screened for mutations in *MYO7A*. A total of 18 of 56 subjects (32.1%) were observed to have one or two *CDH23* variants that are presumed to be pathologic. Twenty one different pathologic genome variants were observed of which 15 were novel. Out of a total of 112 alleles, 31 (27.7%) were considered pathologic. Based on our results it is estimated that about 20% of patients with Usher syndrome type I have *CDH23* mutations. © 2008 Wiley-Liss, Inc.

KEY WORDS: Usher syndrome, CDH23, Cadherins, mutation, Retinitis Pigmentosa, Hearing Loss

INTRODUCTION

Usher syndrome is an autosomal recessive disorder recognized as the most frequent cause of deaf-blindness; it is estimated to account for ~10% of the pediatric deaf and hard of hearing (D/HOH) population (Kimberling, 2007). The frequency of Usher syndrome has been estimated to be 3.5/100,000 in Sweden and Finland (Nuutila, 1970; Grondhal, 1987), 3.2/100,000 in Colombia (Tamayo, et al., 1991), 4.4/100,000 in the United States (Boughman, Vernon, and Shaver, 1983), and 4.2/100,000 (Espinos, et al., 1998) in Spain. A most recent report (Sadeghi et al., 2004) from Sweden reported a overall prevalence of 3.3/100,000 with the estimate of the three clinical subtypes being 1.4, 1.6, and 0.3 per 100,000 for type I, II, and III respectively.

The standard classification of Usher syndrome recognizes three distinct clinical categories (Kimberling and Moller, 1995; Smith et al., 1994). Type I is characterized by severe to profound congenital hearing impairment, vestibular dysfunction, and prepubertal onset of the retinal degeneration; type II is manifested by moderate to

Received 8 August 2007; accepted revised manuscript 19 December 2007.

DOI: 10.1002/humu.20761

severe hearing impairment, normal vestibular function, and teenage onset of retinal degeneration. Type III, the least common form of Usher syndrome, presents with progressive hearing loss and a variable retinal and vestibular phenotype.

At least six different loci are associated with the more severe, type I syndrome. These USH1 genes have been mapped to chromosomes 10q21.1(1F), 10q22.1(1D), 11q13.5(1B), 11p15.1(1C), 17q23-25(1G), and 21q21(1E) (see the Hereditary Hearing Loss Homepage http://webhost.ua.ac.be/hhh/). There are no reported consistent clinical differences between the five Usher type I genetic subtypes, so they are differentiated primarily on the basis of either linkage analysis in linkage informative families or mutational analysis of the genes involved.

Five USH1 genes have been identified so far. Defects in myosin VIIa, harmonin, cadherin 23, protocadherin 15, and sans are responsible for causing Usher syndrome type I subtypes B C, D, F and G, respectively (Weil et al., 1995; Bitner-Glindzicz et al., 2000; Verpy et al., 2000; Ahmed et al., 2001; Alagramam et al., 2001; Bolz et al., 2001; Bork et al., 2001; Weil et al., 2003).

USH1D (MIM# 601067) was first mapped to the long arm of chromosome 10 (Wayne et al. 1996), a chromosomal region that also contained *DFNB12* (MIM# 601386), a nonsyndromic deafness locus (Chaib et al. 1996). *CDH23* (MIM# 605516) was subsequently identified as the gene responsible (Bolz et al., 2001; Bork et al., 2001). It was later recognized that mutations in *CDH23* cause both Usher syndrome and nonsyndromic deafness (Astuto et al., 2002). Only missense mutations of *CDH23* have been observed in families with nonsyndromic hearing loss, whereas nonsense, frame shift, splice site, and missense mutations have been observed in families with Usher 1D (Astuto et al., 2002). No instance of isolated autosomal recessive retinitis pigmentosa has been reported as due to pathologic variation in *CDH23*.

The murine ortholog is located on murine chromosome 10 and the mutant forms of murine *CDH23* give rise to waltzer phenotype. The waltzer mouse exhibits deafness and vestibular dysfunction and shows disorganized, splayed stereocilia (Di Palma et al., 2001; Holme et al., 2002). A strain-specific *CDH23* is likely responsible for the modifier of deaf waddler (*mdfw*) and age-related hearing loss locus (*ahl*) (Noben-Trauth et al., 2003; Johnson et al,. 2007).

CDH23 has 69 exons and encodes a predicted 3354 amino acid protein with 27 cadherin extracellular (EC) repeats, a transmembrane domain, and a unique cytoplasmic domain. Each extracellular domain contains cadherin-specific amino acid motifs such as LDRE, DXD, DXNDN, highly conserved in sequence and spacing, that are required for cadherin dimerization and Ca^{2+}-binding (Rowlands et al., 2000). It is known that the cytoplasmic domain can interact with another hair bundle protein, the PDZ domain containing protein known as harmonin (Boeda et al., 2002; Siemens et al., 2002). Mutations in Harmonin are associated with Usher type IC. *CDH23* is a putative calcium-dependent adhesion molecule required for proper morphogenesis of hair bundles of the inner ear neurosensory cells (Frolenkov et al., 2004). Also, recent studies indicated that cadherin 23 is a component of tip links thought to compose mechano- electrical transducer channels of the hair cells (Siemens et al., 2004; Sollner et al., 2004).

In the present study, we report the results of mutation analysis in all 69 exons of the *CDH23* gene in 56 probands from Spain, the United States, and Sweden with Usher syndrome type I who had been previously screened for mutations in *MYO7A*.

MATERIALS AND METHODS

Subjects

A total of 56 probands with Usher syndrome were sampled and studied. Families were collected in Spain (29 families), the United States (27 families), and Sweden (3 families). Subjects were classified as Usher I on the basis of their clinical history and the results of their ophthalmologic, audiometric, and vestibular tests. We refer to families with Usher syndrome Type I as those presenting with profound deafness, RP, and absent vestibular function. In all affected patients, mutations in *MYO7A* were excluded by a previous mutation analysis of that gene. A set of 96 genetically independent normal control samples from both Spain and the USA were studied. The local human-subjects committees approved the present study, and informed consent was obtained from all participants.

Mutation analysis

Genomic DNA was extracted from peripheral blood samples by a Puregene kit (Gentra System). All 69 exons including intron-exon boundaries of the *CDH23* gene were amplified by using polymerase chain reaction (PCR).